HortScience 60(12):2232–2243. 2025. https://doi.org/10.21273/HORTSCI18600-25

Macrogenomic Technology Reveals that Hartz Mycorrhizal Fungicide and Intercropped Garlic Ameliorate Succession Disorders in Continuous Nonheading Chinese Cabbage (*Brassica rapa* L. subsp. *chinensis*)

Fang Wang, Xiaoli Wang, Rong Zhao, Lihua Zhang, Suhua Li, Nan Zhang, and Haozhang Han
College of Materials and Biology, Suqian University, Suqian 223800, China

Keywords. *Brassica rapa* L. subsp. *Chinensis*, *Trichoderma harzianum*, garlic intercropping, metagenome, microbial community structure

Abstract. **Using metagenomic sequencing, we assessed the effects of *Trichoderma harzianum* and garlic intercropping on the growth, soil microbial community, and sustainability of continuous nonheading Chinese cabbage (NHCC; *Brassica rapa* L. subsp. *chinensis*). Four treatments were evaluated: NHCC monoculture control treatment; NHCC monoculture inoculated with *T. harzianum* (T1); NHCC–garlic intercropping with water (T2); and NHCC–garlic intercropping inoculated with *T. harzianum* (T3). Growth parameters, physiological indices, soil quality, and rhizosphere microbial composition were analyzed. The results showed that T1, T2, and T3 significantly altered fungal and bacterial community composition in NHCC rhizosphere soil, and that T1 increased the relative abundance of *Lysobacter antibioticus* and decreased the relative abundance of *Fusarium oxysporum*. The T2 treatment increased the relative abundances of *Dactylellina haptotyla*, *Bacillus subtilis*, *Nitrospira japonica*, and *Lysobacter antibioticus* as well as suppressed *Macrophomina phaseolina*. The T3 treatment increased the relative abundances of *Pochonia chlamydosporia*, *Bacillus subtilis*, and *Nitrospira japonica* as well as decreased the relative abundances of *Macrophomina phaseolina* and *Fusarium oxysporum*. The Kyoto Encyclopedia of Genes and Genomes analysis revealed heightened enrichment of metabolism-related microorganisms in T2 and T3. The T1 treatment upregulated phoD (alkaline phosphatase), nirK, and nirS (nitrate reduction). The T2 treatment increased phoD, narG (nitrate reduction), nirS, and amoA (ammonia oxidation). The T3 treatment exhibited the broadest activation, elevating phoD, narG, nirK, nirS, and amoA. The T1, T2, and T3 treatments significantly increased soil available nitrogen and soil available potassium content. The T2 and T3 treatments increased exchangeable calcium (Ca^{2+}). The T3 treatment uniquely elevated available phosphorus. Organic matter, total phosphorus, and total potassium remained unaffected. All treatments improved NHCC leaf length, width, and fresh weight; T2 and T3 increased plant height; and T3 enhanced root length. The T1, T2, and T3 treatments reduced leaf soluble protein, superoxide dismutase, and malondialdehyde. The T2 and T3 treatments significantly increased the content of soluble sugar in leaves and significantly decreased the content of peroxidase. The T3 treatment significantly increased the content of chlorophyll in leaves. These results demonstrate that *T. harzianum*, NHCC–garlic intercropping, and NHCC–garlic intercropping inoculated with *T. harzianum* enhance NHCC growth, soil quality, and beneficial microbiota while suppressing pathogens. Furthermore, NHCC–garlic intercropping inoculated with *T. harzianum* yielded a superior effect, while the effect of NHCC monoculture inoculated with *T. harzianum* had the weakest effect.**

Nonheading Chinese cabbage (NHCC) (*Brassica rapa* L. subsp. *chinensis*), also known as Chinese cabbage or rapeseed, is a subspecies of *Brassicaceae* in the Brassicaceae family. It originated in China and is characterized by its short growth cycle, high yield, adaptability, resistance to storage and transportation, and cost-effectiveness. These traits have led to its widespread cultivation not only in China and Southeast Asia but also globally, where it is recognized as a key leafy vegetable (Li et al. 2020). Rich in vitamins, amino acids, and minerals, NHCC is valued for its role in disease prevention and metabolic regulation, thus contributing to its high consumer demand (Wang et al. 2022; Zhou et al. 2022). Suqian, located in northern Jiangsu Province, China, lies within a warm temperate monsoon climate zone, which provides optimal environmental conditions for the development of the vegetable industry (Wang et al. 2024). Because of the limitations of arable land and growing conditions, continuous cultivation has become a common growing method. However, continuous cropping of NHCC has been associated with declines in yield and quality, thus posing challenges to the industry's sustainable development. Recent efforts to address soil ecological security have prioritized the use of microbial fungicides and alterations to cropping patterns as potential strategies for mitigating the persistent issue of continuous obstacles.

Microbial agents can enhance the physicochemical properties of continuous cropping soil, inhibit the propagation of soil pathogens, improve the structure of soil microbial communities, enhance the absorption of soil nutrients by plants, and strengthen the resistance of plants. Consequently, the quality and yield of plants can be improved (Chen et al. 2021; Elnahal et al. 2022; Jaber and Enkerli 2016; Wang et al. 2024). Nitrogen-fixing bacteria, *Bacillus*, lactic acid bacteria, actinomycetes, and *Trichoderma* are the most commonly used microbial inoculant strains. Of these, *Trichoderma* is the most widely used (Al-Shuaibi et al. 2024; Cao et al. 2022; Erazo et al. 2021; Patkowska et al. 2020). Al-Shuaibi et al. (2024) found that *Trichoderma ghanense* and *Trichoderma citrinoviride* inhibited the reproduction of *Pythium aphanidermatum* and promoted the growth of cucumber. Similarly, Erazo et al. (2021) observed that *Trichoderma harzianum* application reduced the peanut brown root rot incidence and stimulated plant growth. Cao et al. (2022) further demonstrated that biochar combined with Trichoderma enhanced soil bacterial diversity, improved soil physicochemical properties, and increased root vitality. Patkowska et al. (2020) demonstrated that *T. harzianum* significantly increases the number of beneficial bacteria such as *Bacillus* and *Pseudomonas* in carrot rhizosphere soil. Scientifically optimized planting patterns can modify the soil microenvironment and mitigate continuous cropping challenges (Xia et al. 2016; Zeng et al. 2020).

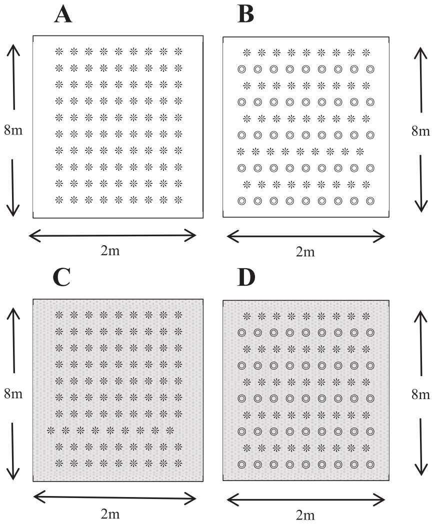

Fig. 1. Planting patterns. (**A**) Nonheading Chinese cabbage (NHCC) monoculture control treatment (CK). (**B**) NHCC–garlic intercropping with water (T2). (**C**) NHCC monoculture inoculated with *T. harzianum* (T1). (**D**) NHCC–garlic intercropping inoculated with *T. harzianum* (T3). *NHCC. ○Garlic.

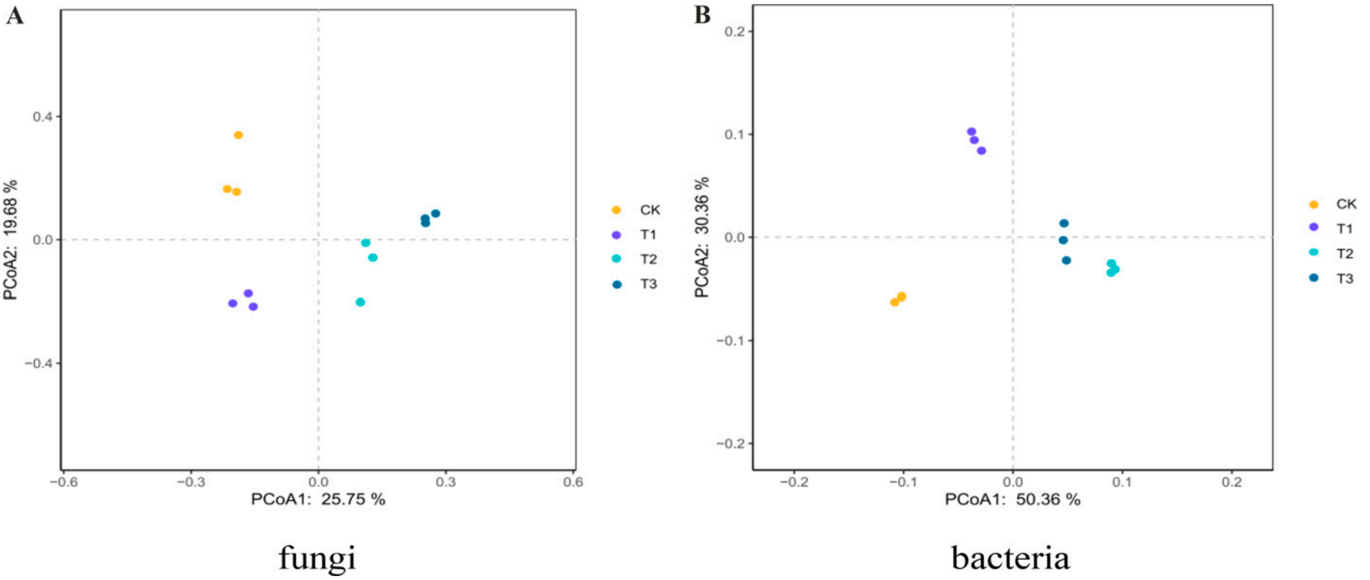

Fig. 2. Principal coordinate analysis of the rhizosphere soil microbial community structure.

Kermah et al. (2017) reported that maize–grain legume intercropping enhances crop yield and improves soybean nitrogen fixation efficiency. Similarly, Xiao et al. (2012) observed that cucumber–garlic intercropping improves soil biological conditions and alleviates cucumber continuous cropping obstacles. Zhou et al. (2011) further confirmed that intercropping cucumber with onion or garlic boosts productivity and enhances soil quality.

In this study, metagenomic technology was used to investigate the effects of *T. harzianum* and NHCC–garlic intercropping on rhizosphere microbial community structure and function. Additionally, we evaluated their impacts on NHCC growth indices, physiological parameters, and rhizosphere soil nutrient dynamics.

Materials and Methods

Experimental materials and experimental design. The experiment was conducted from Mar 2024 to May 2024 at the facility's horticultural cultivation base in Suqian College, Jiangsu Province (118°262′N, 33°850′E), where NHCC was continuously planted for 5 years. The physicochemical properties of the soil were as follows: organic matter, 25.25 g·kg^{-1}; total phosphorus, 0.86 g·kg^{-1}; total potassium, 10.48 g·kg^{-1}; available nitrogen, 74.26 mg·kg^{-1}; available phosphorus, 25.85 mg·kg^{-1}; available potassium, 47.22 mg·kg^{-1}; and exchangeable calcium, 1408.82 mg·kg^{-1}. The seeds of NHCC ('Lvguan') were sourced from Shouguang Yinuo Agricultural Science and Technology Ltd. (Shandong, China), garlic bulbs were sourced from Anhui Jiuqi Seedling Technology Ltd. (Anhui, China), and *T. harzianum*

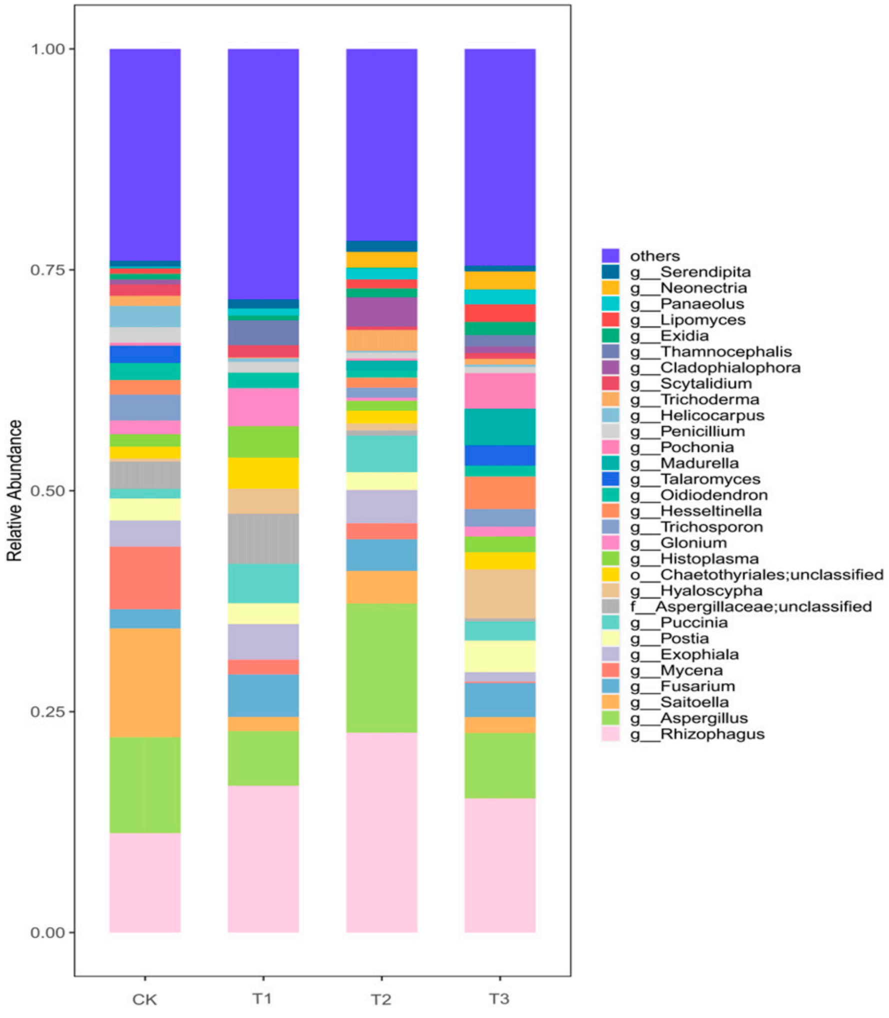

Fig. 3. Relative abundance histogram of fungi at the genus level.

Received for publication 21 Mar 2025. Accepted for publication 25 Sep 2025.

H.H. developed concepts and designed the study. F.W., X.W., R.Z., and L.Z. implemented the study. F.W. analyzed and interpretated data and wrote the manuscript. H.H. supervised data analysis and interpretation. H.H., S.L., and N.Z. revised the manuscript.
This work was supported by the Suqian Sci Tech Program (grant no. S202310).
H.H. and F.W. are the corresponding authors. E-mail: 21011@squ.edu.cn and 23068@squ.edu.cn.

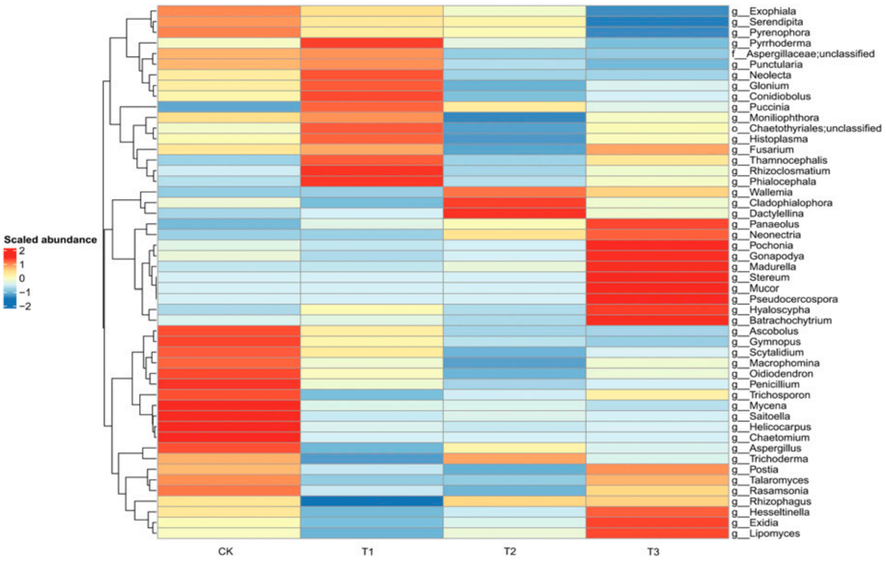

Fig. 4. Cluster heat map of fungi at the genus level.

was sourced from T-22 inoculant [$\geq 5 \times 10^9$ colony-forming units (CFU)/g] from Shandong Weifang Nuojin Agrochemical Ltd. (Shandong, China).

The following four treatments were used in the experiment: NHCC monoculture control treatment (CK); NHCC monoculture inoculated with *T. harzianum* (T1); NHCC–garlic intercropping with water (T2); and NHCC–garlic intercropping inoculated with *T. harzianum* (T3). Each treatment was replicated three times in randomized 2- × 8-m plots. Plants were spaced 20 cm apart (Fig. 1) and sown on 15 Mar 2024. Ten days postplanting, *T. harzianum* suspension (1:600 dilution) was applied to T1 and T3 plots. Routine field maintenance was performed, and NHCC was harvested on 24 Apr 2024.

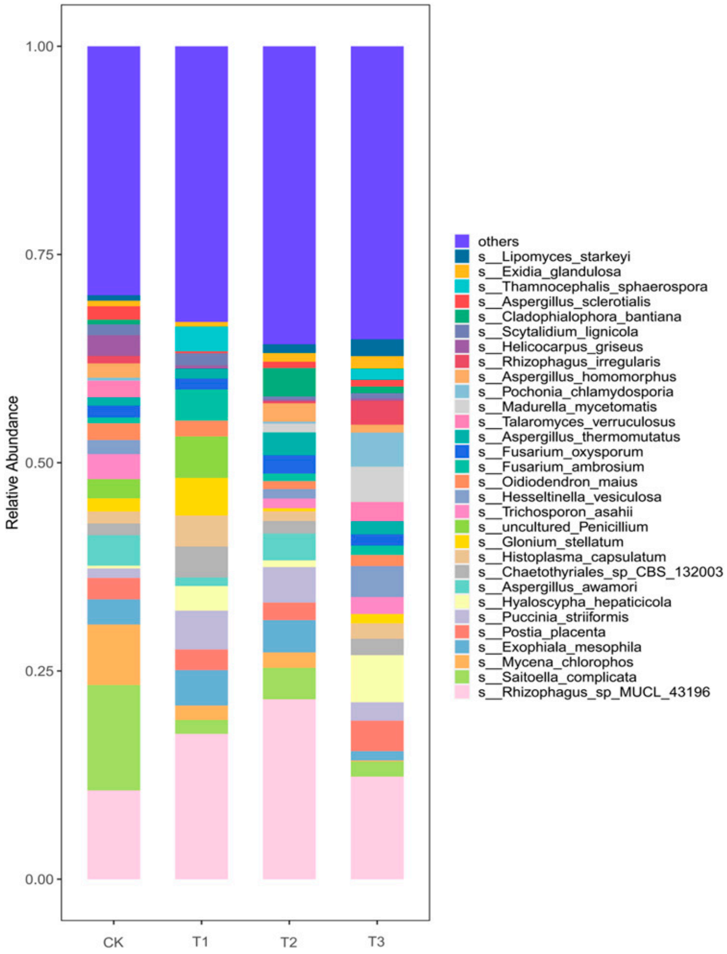

Fig. 5. Relative abundance histogram of the fungal species level.

Leaf selection and soil collection methods. On 18 Apr 2024, leaf and soil samples were collected from NHCC. Five NHCCs were randomly selected from each treatment, and the plant height, fresh weight, and longest root length were measured. The fourth leaf from the top to the bottom was selected to measure leaf length, leaf width, chlorophyll content, soluble sugar content, soluble protein content, peroxidase (POD) activity, superoxide dismutase (SOD) activity, and malondialdehyde (MDA) content. Soil samples were collected using the "root-shaking method." After uprooting the plants, loosely adhered soil was removed by gentle shaking, and soil that was tightly adhering to the roots was retained (Ren et al. 2020). The rhizosphere soil of 10 nonheading cabbages was randomly collected from each treatment. The soil samples were immediately stored on dry ice and transported to the laboratory. Samples were sieved (2-mm mesh) and divided into two aliquots: one stored at 4 °C for the soil physicochemical analysis and the other stored at –80 °C for microbial community characterization (Zhang et al. 2021).

Determination of growth and physiological indexes of NHCC. Plant height, root length, leaf length, and leaf width were measured using a calibrated ruler. Fresh weight was determined with an electronic balance (±0.01 g precision). Chlorophyll content (Ahmad et al. 2022), soluble sugar (Irani et al. 2021), and MDA (Xia et al. 2016) were quantified via ultraviolet–Vis spectrophotometry. Soluble protein was assayed using the Coomassie brilliant blue G-250 method (Ahmad et al. 2022). The POD activity was measured via the guaiacol oxidation method (Ahmad et al. 2022), and SOD activity was determined using the nitroblue tetrazolium chloride (NBT) reduction assay (Ahmad et al. 2022).

Determination of soil physical and chemical properties. Soil organic matter was analyzed by potassium dichromate volumetric titration (Yang et al. 2023). Total potassium and total phosphorus were quantified using NaOH fusion followed by flame photometry (Gao et al. 2019) and molybdenum-antimony anticolorimetric methods (Gao et al. 2019), respectively. Available nitrogen was measured using the alkali hydrolysis diffusion method (Chen et al. 2016). Available phosphorus was measured using molybdenum-antimony anti-colorimetry (Yang et al. 2023). Available potassium was measured using ammonium acetate flame photometry (Yang et al. 2023). Exchangeable calcium (Ca^{2+}) was determined using ammonium acetate extraction followed by atomic absorption spectrometry (Han et al. 2019).

Soil microbial community macrogenomic determination. Metagenomic sequencing was performed using the Illumina NovaSeq high-throughput sequencing platform (Shanghai Zhongke New Life Biotechnology Co., Ltd.,

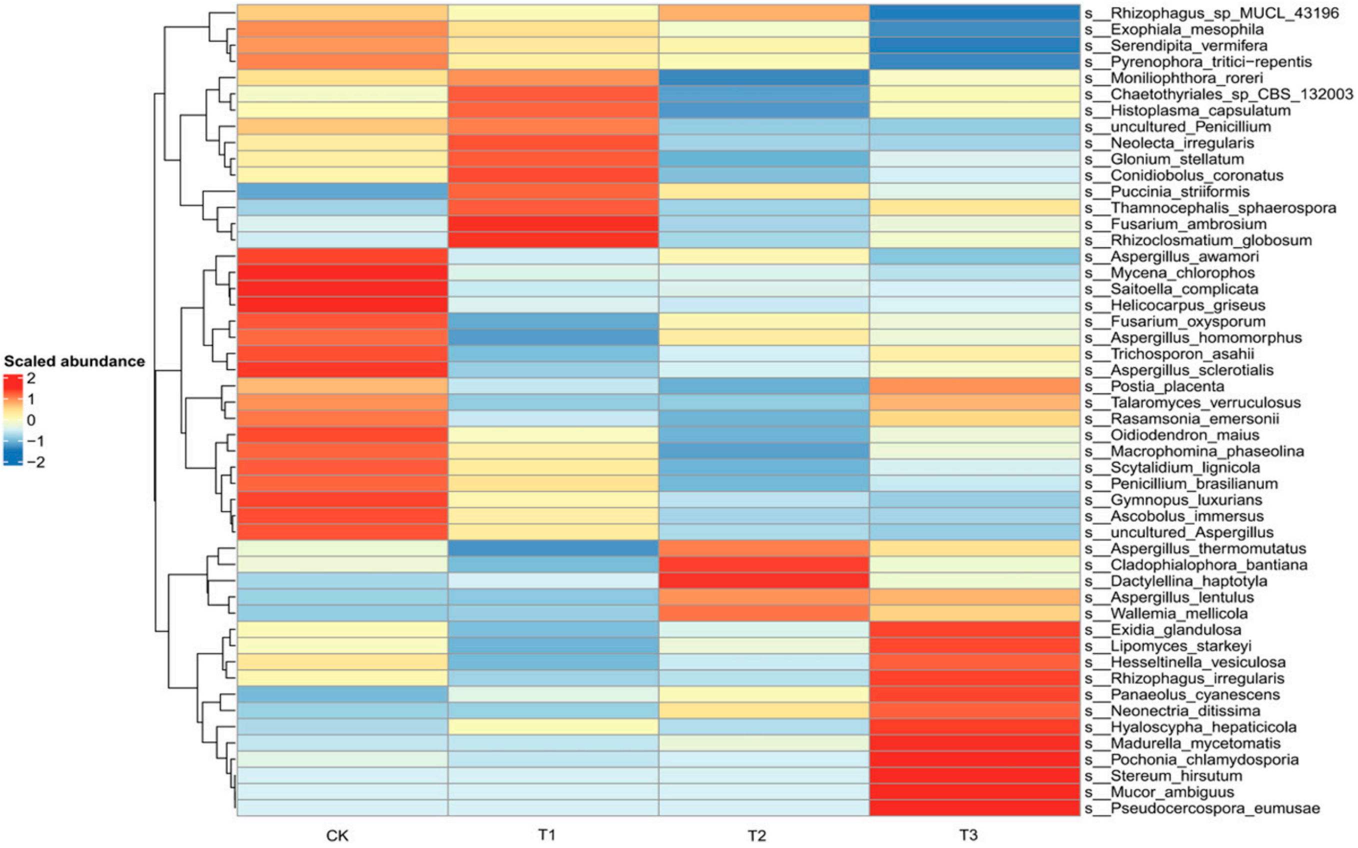

Fig. 6. Cluster heat map of the fungal species level.

Shanghai, China) to obtain metagenomic raw data of fungi and bacteria in the rhizosphere soil of NHCC. The raw data were split and quality-clipped to obtain valid data. Valid data were assembled using MEGAHIT(a software tool for efficient assembly of metagenomic data) (Li et al. 2015; Li et al. 2016) and De Bruijn graph-based splicing software; contigs longer than 500 bp were retained for the downstream analysis. The spliced contigs sequence was open reading frame (ORF) predicted by Prodigal software (protein-coding gene prediction software) and translated into an amino acid sequence (Hyatt et al. 2010). The ORF prediction results of all soil samples were deredundified using CD-HIT software (Fu et al. 2012) to obtain a nonredundant initial gene catalog, which was clustered with 95% identity and 90% coverage, and the longest sequence was selected as the representative sequence. Clean reads of each sample were aligned with nonredundant overlapping cluster sequences using bowtie2 software to calculate gene abundance (Langmead and Salzberg 2012). The nonredundant genes were aligned to the EggNOG database and the carbohydrate-active enzymes (CAZy) database using DIAMOND software (Cantarel et al. 2009). The annotations with e $<$ 1e-5 were selected to screen the proteins with the highest sequence similarity, yielding Kyoto Encyclopedia of Genes and Genomes (KEGG) and CAZy annotations. Community composition, abundance clustering, and a principal coordinate analysis were conducted based on taxonomic and functional profiles. Then, LEfSe (an analytical tool for discovering and interpreting differences in high-dimensional data biomarkers) was used to identify differentially abundant taxa and functions across treatments (Villar et al. 2015).

Data analysis. Microsoft Excel 2016 (Redmond, WA, USA) was used for data organization, and IBM SPSS 26.0 was used for statistical analysis. Differences between treatments were assessed using a one-way analysis of variance (ANOVA), followed by independent-sample t tests. Statistical significance was defined as $P < 0.05$. Results are presented as mean ± standard deviation.

Results

Effects on β diversity of bacteria and fungi. To understand the effects of different treatments on soil microbial community composition, a principal coordinate analysis of soil fungi and bacteria in 12 samples at the species level was performed. The results showed that the microbial structure composition of the four groups was different. Axes 1 and 2 in fungi explained 25.75% and 19.68% of the total variation, respectively, and axes 1 and 2 in bacteria explained 50.36% and 30.36% of the total variation, respectively (Fig. 2). Clear separation of fungal and bacterial communities among CK, T1, T2, and T3 along both axes indicated that all treatments significantly altered the rhizosphere microbial composition.

Effects on fungal community composition. The relative abundance of soil fungal communities at the genus level revealed a higher abundance of the Rhizophagus, *Aspergillus*, Saitoella, *Fusarium*, and Mycena in CK, T1, T2, and T3 (Fig. 3). The fungi cluster analysis heat map at the genus level of different treatments is shown in Fig. 4. In T1, the relative abundances of *Puccinia*, *Thamnocephalis*, *Rhizoclosmatium*, and *Phialocephala* were significantly higher than those in CK, while those of *Lipomyces*, *Exidia*, *Hesseltinella*, *Rhizophagus*, *Trichosporon*, and *Macrophomina* were significantly lower than those in CK. In T2, the relative abundances of *Wallemia*, *Cladophialophora*, and *Dactylellina* were significantly higher than those of CK, and those in *Ascobolus*, *Gymnopus*, *Scytalidium*, *Macrophomina*, *Oidiodendron*, *Penicillium*, *Trichosporon*, *Mycena*, *Saitoella*, *Helicocarpus*, *Chaetomium*, *Moniliophthora*, *Histoplasma*, and *Fusarium* were significantly lower than those in CK. In T3, the relative abundances of *Panaeolus*, *Neonectria*, *Pochonia*, *Gonapodya*, *Madurella*, *Stereum*, *Mucor*, *Pseudocercospora*, *Hyaloscypha*, and *Batrachochytrium* were significantly higher than those in CK, while the relative abundances of *Exophiala*, *Serendipita*, *Pyrenophora*, *Macrophomina*, *Oidiodendron*, *Penicillium*, *Mycena*, and *Saitoella* were significantly lower than those in CK.

At the species level, the relative abundance of soil fungal communities across treatments (CK, T1, T2, T3) revealed higher proportions of

Rhizophagus sp. MUCL 43196, *Saitoella complicata*, *Mycena chlorophos*, *Exophiala mesophila*, and *Postia placenta* (Fig. 5). Cluster analysis heat maps of fungal communities at the species level are shown in Fig. 6. In T1, the relative abundances of *Chaetothyriales* sp CBS 132003, *Histoplasma capsulatum*, *Neolecta irregularis*, *Glonium stellatum*, *Conidiobolus coronatus*, *Puccinia striiformis*, *Thamnocephalis sphaerospora*, *Fusarium ambrosium*, and *Rhizoclosmatium globosum* were significantly higher than those in CK, while those of *Fusarium oxysporum*, *Aspergillus homomorphus*, *Trichosporon asahii*, *Aspergillus sclerotialis*, *Postia placenta*, *Talaromyces verruculosus*, and *Rasamsonia emersonii* were significantly lower than those in CK. The T2 treatment revealed increased relative abundances of *Aspergillus thermomutatus*, *Cladophialophora bantiana*, *Dactylellina haptotyla*, *Aspergillus lentulus*, and *Wallemia mellicola*, and reduced abundances of *Postia placenta*, *Talaromyces verruculosus*, *Rasamsonia emersonii*, *Oidiodendron maius*, *Macrophomina phaseolina*, *Scytalidium lignicola*, *Penicillium brasilianum*, *Gymnopus luxurians*, *Ascobolus immerses*, and *uncultured Aspergillus.* Similarly, T3 showed increased abundances of *Exidia glandulosa*, *Lipomyces starkeyi*, *Hesseltinella vesiculosa*, *Rhizophagus irregularis*, *Panaeolus cyanescens*, *Neonectria ditissima*, *Hyaloscypha hepaticicola*, *Madurella mycetomatis*, *Pochonia chlamydosporia*, *Stereum hirsutum*, *Mucor ambiguous*, and *Pseudocercospora eumusae*, and decreased abundances of *Aspergillus awamori*, *Mycena chlorophos*, *Saitoella complicate*, *Helicocarpus griseus*, *Fusarium oxysporum*, *Aspergillus homomorphus*, *Oidiodendron maius*, *Macrophomina phaseolina*, *Scytalidium lignicola*, *Penicillium brasilianum*, *Gymnopus luxurians*, *Ascobolus immerses*, and *uncultured Aspergillus*.

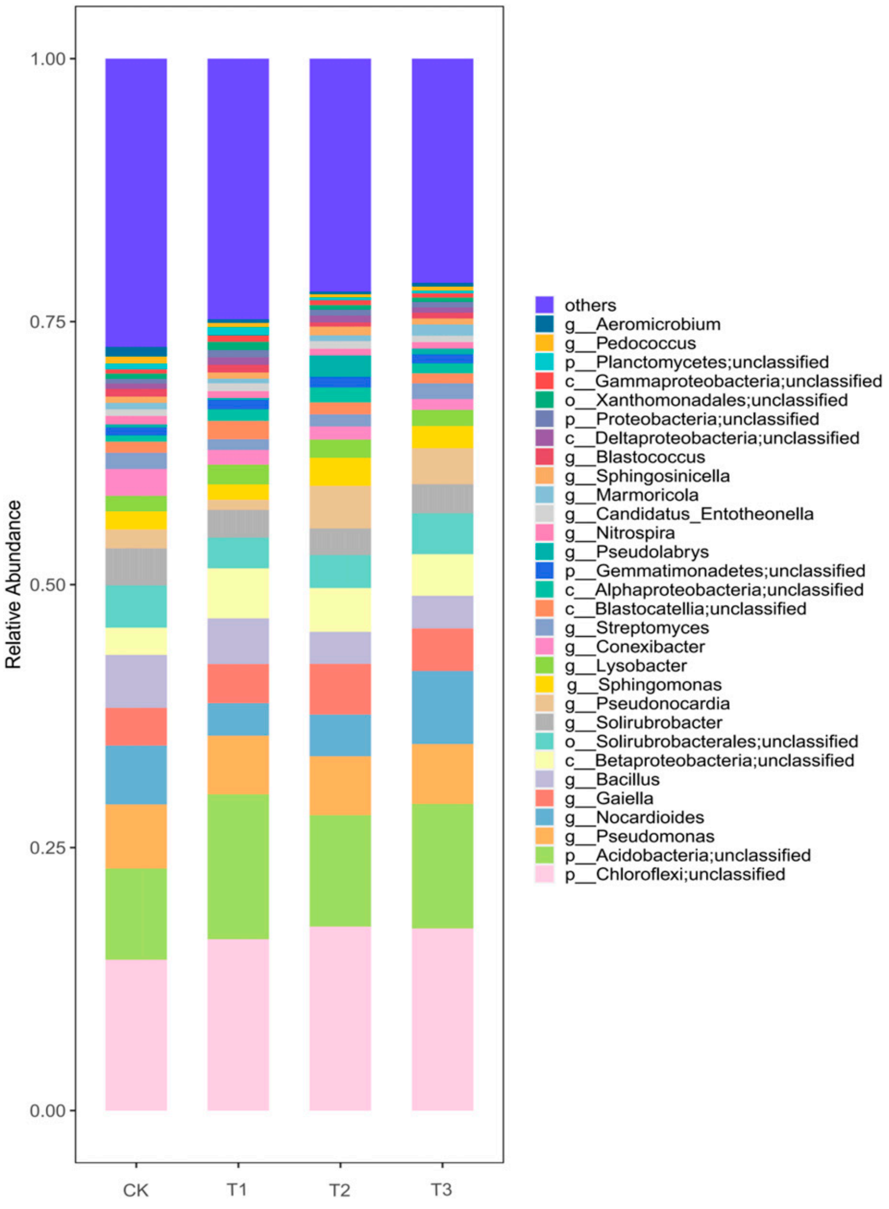

Fig. 7. Relative abundance histogram of bacteria at the genus level.

Effects on bacterial community composition. At the genus level, soil bacterial communities in CK, T1, T2, and T3 showed higher relative abundances of *Chloroflexi* (unclassified), *Acidobacteria* (unclassified), *Pseudomonas*, *Nocardioides*, *Gaiella*, and *Bacillus* (Fig. 7). Bacterial cluster analysis heat maps are shown in Fig. 8. The T1 treatment exhibited increased abundances of *Nitrospira*, *Chloroflexi* (unclassified), *Verrucomicrobia* (unclassified), and *Candidatus Entotheonella*, and decreased abundances of *Nocardioides*, *Actinobacteria* (unclassified), *Solirubrobacterales* (unclassified), and *Streptomyces*. In T2, the relative abundances of *Nitrospira*, *Sphingosinicella*, *Bradyrhizobium*, *Pseudolabrys*, *Gaiella*, *Lysobacter*, *Amycolatopsis*, *Pseudonocardia*, *Sphingomonas*, and *Bacillus* were significantly higher than those in CK. The relative abundances of *Solirubrobacter*, *Pedococcus*, *Conexibacter*, *Gemmatimonas*, *Mycobacterium*, *Micromonospora*, *Altererythrobacter*, *Patulibacter*, *Aeromicrobium*, *Agromyces*, *Arthrobacter*, *Geodermatophilus*, and *Blastococcus* were significantly lower than those in CK. In T3, the relative abundances of *Nocardioides*, *Marmoricola*, *Nitrospira*, *Gaiella*, *Lysobacter*, *Pseudonocardia*, *Sphingomonas*, and *Bacillus* were significantly higher than those in CK, and the relative abundances of *Solirubrobacter*, *Conexibacter*, *Gemmatimonas*, and *Mycobacterium* were significantly lower than those in CK.

The relative abundances of soil bacterial communities at the species level revealed higher proportions of *Acidobacteria bacterium*, *Chloroflexi bacterium*, *Bacillus subtilis*, and *Gaiella occulta* in CK, T1, T2, and T3 (Fig. 9). Cluster analysis heat maps at the species level demonstrated distinct microbial profiles across treatments (Fig. 10). In T1, the relative abundances of *Acidobacteria bacterium*, *Verrucomicrobia bacterium*, *Lysobacter antibioticus*, *Proteobacteria bacterium*, *Gemmatimonadetes bacterium*, *Alphaproteobacteria bacterium*, *Anaerolineae bacterium*, *bacterium HR12*, *Xanthomonadales bacterium*, *Blastocatellia bacterium*, *uncultured bacterium*, *Chloroflexi bacterium*, and *bacterium* were significantly higher than those in CK, while the relative abundances of *Pseudonocardiales bacterium*, *Pseudomonas putida*, and *Actinobacteria bacterium* RBG 16 67 10 were reduced. In T2, the relative abundances of *Pseudomonas monteilii, Gaiella occulta, Bacillus subtilis*, *Pseudonocardia acaciae*, *Nitrospira japonica*, *Sphingomonas* sp URHD0057, *Verrucomicrobia bacterium*, *Lysobacter antibioticus*, *Proteobacteria bacterium*, *Gemmatimonadetes bacterium*, and *Alphaproteobacteria bacterium* were significantly higher than those in CK, whereas the relative abundances of *Acidimicrobiales bacterium*, *Conexibacter woesei*, *Solirubrobacter pauli*, *Solirubrobacter* sp URHD0082, *Solirubrobacter soli*, *Pedococcus cremeus*, *Conexibacter* sp Seoho 28, *Solirubrobacterales bacterium*, and *Altererythrobacter* sp Root672 were decreased. The T3 treatment exhibited significantly higher abundances of *Gaiella occulta*, *Sphingosinicella* sp CPCC 101087, *Bacillus subtilis*, *Chloroflexi bacterium* RBG_16_72_14, *Chloroflexi bacterium* RBG_16_69_14, *Chloroflexi bacterium* GWC2_73_18, *Pseudonocardia acaciae*, *Nitrospira japonica*, *Sphingomonas* sp

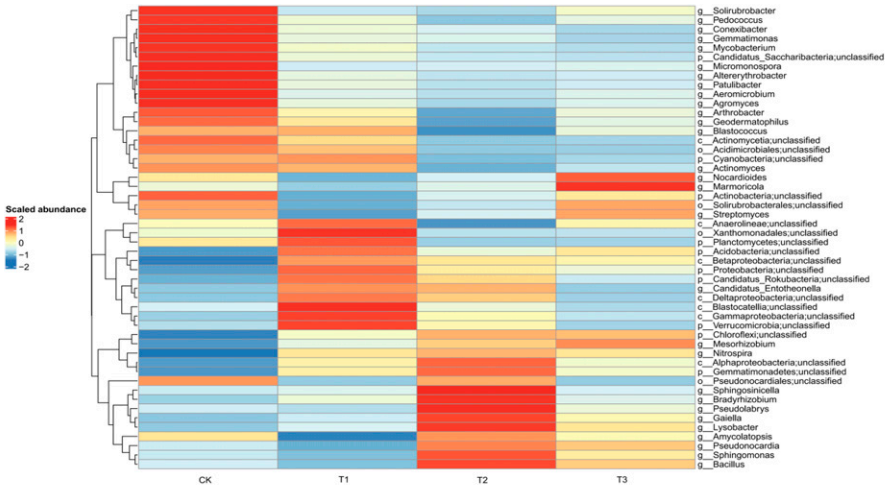

Fig. 8. Cluster heat map of bacteria at the genus level.

URHD0057, *Nocardioides iriomotensis*, *Pseudomonas sihuiensis*, and *Nocardioides ganghwensis* than those in CK, but lower relative abundances of *Pseudonocardiales bacterium*, *Acidimicrobiales bacterium*, *Conexibacter woesei*, *Solirubrobacter pauli*, *Solirubrobacter* sp URHD0082, and *Solirubrobacter soli*.

KEGG function prediction. A KEGG pathway analysis was performed to assess functional differences in microbial communities across treatments. Significant functional variations were observed at level 2 (Fig. 11). The LEfSe analysis identified the following treatment-specific functional traits (Fig. 12): CK-enriched microbes were associated with endocrine system functions, replication/repair, transport/catabolism, and immune system activity. The T1-enriched microbes exhibited roles in cellular community (prokaryotes), signal transduction, antimicrobial drug resistance, and transcription. The T2-enriched microbes were linked to amino acid metabolism, carbohydrate metabolism, cell growth/death, motility, and cancer-specific pathways. The T3-enriched microbes primarily contributed to glycan biosynthesis, cellular community (eukaryotes), secondary metabolite biosynthesis, and terpenoid/polyketide metabolism. Collectively, T2 and T3 showed stronger enrichment of metabolism-related functions.

CAZy function annotation of soil metagenome. The CAZy family is closely related to carbohydrate metabolism. In this work, the CAZy database was used to analyze the metagenomic data of rhizosphere soil across different treatment groups. The results revealed glycoside hydrolases (GHs) as the most abundant functional group in rhizosphere soil metagenomes, followed by glycosyltransferases (GTs) (Fig. 13). Dominant GH genes included GH13, GH3, GH31, GH23, and GH5, while GT2, GT4, GT51, GT35, GT20, and GT28 topped GTs. The LEfSe analysis indicated the following distinct enrichment patterns: GT2, GH39, GT26, and GH32 were CK-associated; GH3, GH51, GH26, GH19, GH105, GT25, and GH47 dominated T1; GT39, GH15, GT9, GH57, GH102, GT87, PL11, and GT85 characterized T2; and GH13, GT4, CBM48, GT81, GT35, PL8, PL4, GT8, GT17, GH27, and GT14 were enriched in T3 (Fig. 14). Overall, T1, T2, and T3 enhanced carbohydrate metabolism-related gene abundance compared with CK, with T3 exhibiting the highest enrichment.

Effects on functional genes related to nitrogen and phosphorus nutrient cycling in rhizosphere microorganisms. The abundances of differentially expressed functional genes associated with nitrogen and phosphorus nutrient cycling in the four treatment groups are shown in Table 1. The K01113 gene (alkaline phosphatase) exhibited significantly higher abundance in T1, T2, and T3 compared with that in CK. The ammonia oxidation-related K10944 gene was markedly elevated in T2 and T3 relative to that in CK and T1. Among nitrite reduction genes, K00370 abundance was significantly higher in T2 and T3 than in CK and T1, while K00368 showed greater abundance in T1 and T3 compared with that in CK and T2. The K15864 gene was significantly enriched in T1, T2, and T3 compared with CK.

Effects on soil nutrients of NHCC. As shown in Table 2, there were no significant differences in soil organic matter, total phosphorus, and total potassium contents among CK, T1, T2, and T3. Compared with CK, the soil available nitrogen content of T1, T2, and T3 increased significantly by 11.75%, 23.07%, and 31.69%, respectively. There was no significant difference between the available phosphorus content of CK and that of T1 and T2. The soil available phosphorus content of T3 was significantly increased by 37.58% compared with that of CK. Compared with CK, T1, T2, and T3 significantly increased soil available potassium by 8.63%, 11.26%, and 10.83%, respectively. Exchangeable calcium was elevated by 4.54% and 8.00% in T2 and T3, respectively, with no significant changes in T1.

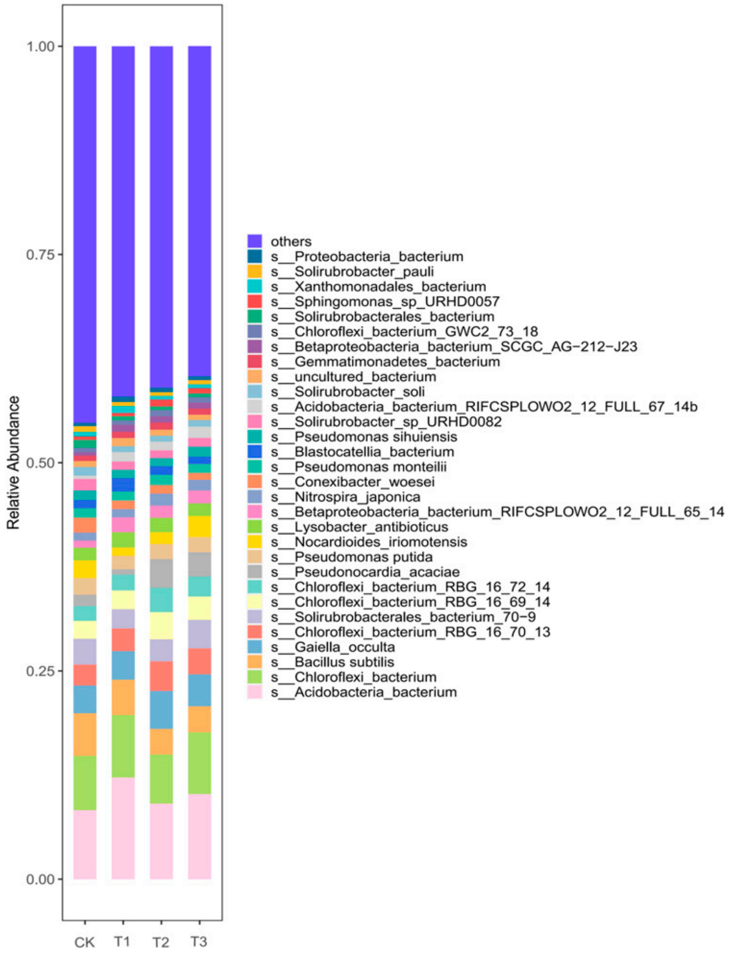

Fig. 9. Relative abundance histogram of the bacteria species level.

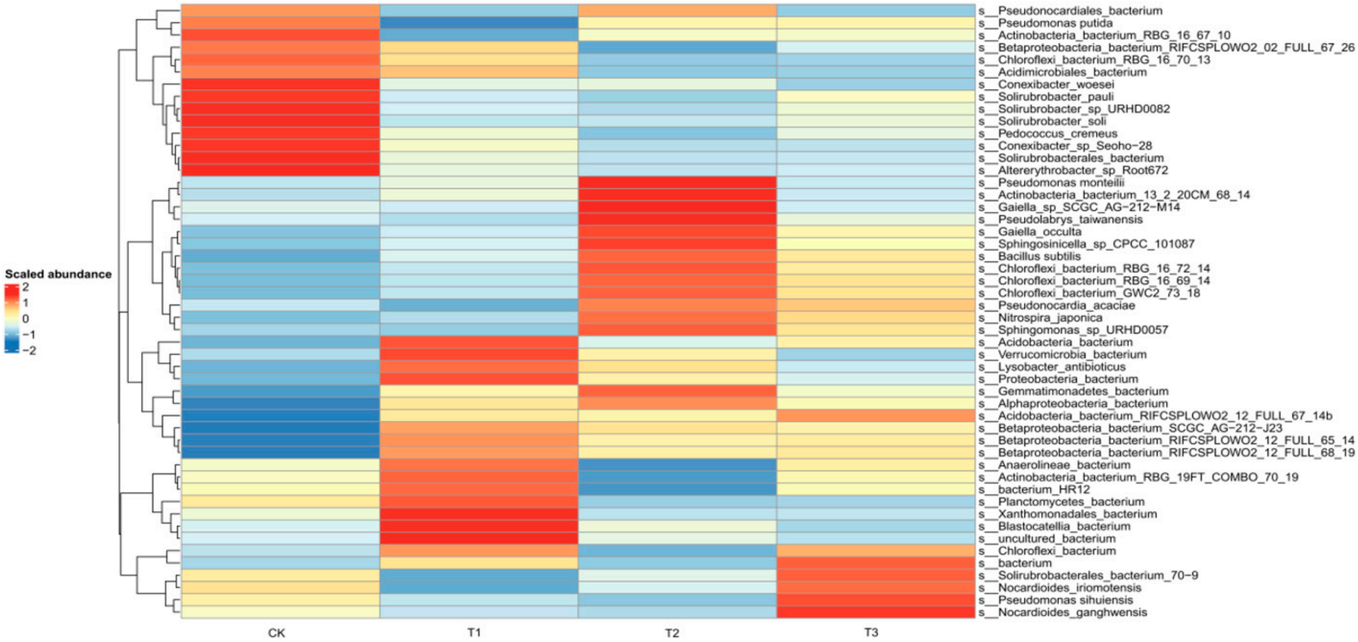

Fig. 10. Cluster heat map of the bacteria species level.

Effects on the growth of NHCC. Growth metrics are detailed in Table 3. Plants in T3 and T2 were significantly taller than those in CK, while those in T3 were significantly taller than those in T2. Maximum root length in T3 was greater than that in CK, but it did not differ from that in T1 or T2. Leaf length had the following order: T3 > T2 > T1 > CK. Leaf width in T3 exceeded that in all other groups, with T1 and T2 surpassing CK. Fresh weight in T3 was higher than that in CK and T1, but comparable to that in T2. These results indicate that all treatments enhanced growth, with T3 demonstrating the strongest effect and T1 demonstrating the weakest effect.

Effects on physiological indexes of NHCC. As shown in Table 4, the chlorophyll content of T3 was significantly higher than that in CK and T1, increasing by 14.71% and 13.59%, respectively, and showed no significant difference with T2. There was no significant difference in soluble sugar content between CK and T1 and between T2 and T3. The soluble sugar content of T2 and T3 was significantly increased by 58.54% and 43.55%, respectively, compared with that of CK. Additionally, T1,

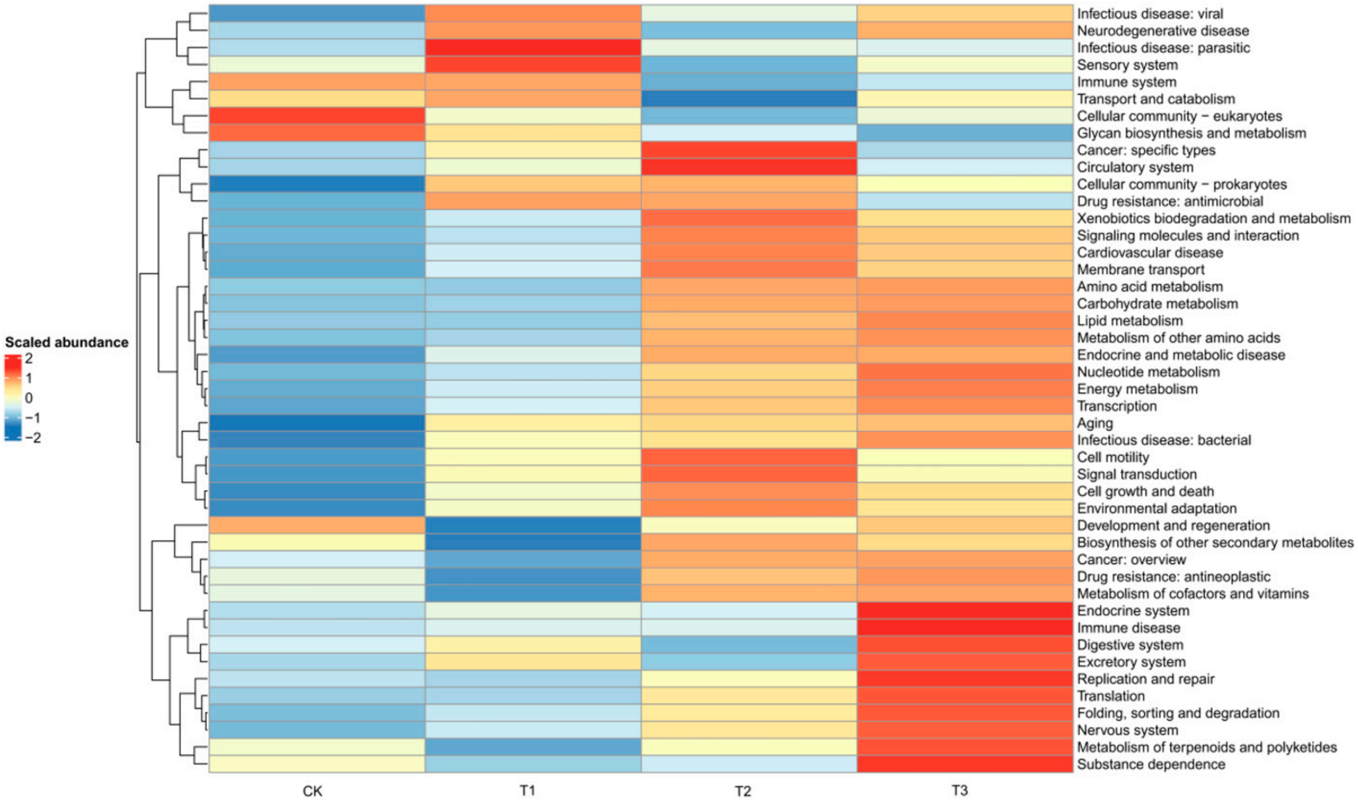

Fig. 11. Heat map of the Kyoto Encyclopedia of Genes and Genomes (KEGG) function prediction at level 2.

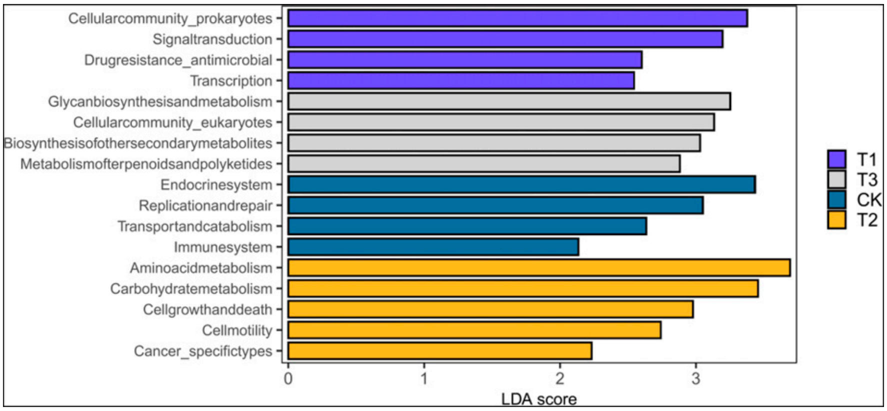

Fig. 12. LEfSe analysis of different functions between groups.

T2, and T3 soluble protein levels were significantly reduced by 12.48%, 16.46%, and 21.67%, respectively, compared with those in CK. There was no significant difference in POD between CK and T1, and no significant difference between T2 and T3. The POD of T2 and T3 was significantly lower than that of CK by 26.12% and 15.09%, respectively. Compared with CK, the SOD contents in T1, T2, and T3 were significantly decreased by 11.09%, 4.66% and 10.65%, respectively. Compared with CK, the MDA contents in T1, T2, and T3 decreased significantly by 26.11%, 7.73%, and 28.20%, respectively.

Discussion

Soil microorganisms are an important part of agricultural ecosystems and play a key role in the decomposition of soil organic matter, nutrient cycling, and nutrient utilization (Hartmann and Six 2023). The NHCC monoculture inoculated with *T. harzianum* increased the relative abundance of *Lysobacter antibioticus* and decreased the relative abundance of *Fusarium oxysporum*. The NHCC–garlic intercropping with water increased the relative abundances of *Dactylellina haptotyla*, *Bacillus subtilis*, *Nitrospira japonica*, and *Lysobacter antibioticus*, and decreased the relative abundance of *Macrophomina phaseolina*. The NHCC–garlic intercropping inoculated with *T. harzianum* increased the relative abundances of *Pochonia chlamydosporia*, *Bacillus subtilis*, and *Nitrospira japonica*, and decreased the relative abundances of *Macrophomina phaseolina* and *Fusarium oxysporum*. *Bacillus subtilis* improves soil structure, synthesizes auxin to enhance plant nitrogen uptake, modulates K/Na ratios to alleviate soil salinity stress, optimizes rhizosphere conditions, and promotes water/nutrient absorption, thereby increasing crop yield (Abbasi et al. 2011; Fang et al. 2021; Hamid et al. 2021; Hashem et al. 2019; Hou et al. 2018; Krey et al. 2011). *Lysobacter antibioticus* is a new type of biocontrol bacteria that has antibacterial characteristics and promotes plant growth (Liu et al. 2022). *Dactylellina haptotyla* and *Pochonia chlamydosporia* are both typical nematode-trapping fungi with efficient lethal potential for soil nematodes (Dos Santos Fonseca et al. 2023; Lei et al. 2023). *Fusarium oxysporum* a soil-borne pathogen, causes Fusarium wilt and root rot across plant developmental stages (Boulahouat et al. 2023), while *Macrophomina phaseolina* infects more than 500 plant species, inducing stem rot, root rot, and seedling blight (Marquez et al. 2021). *Nitrospira japonica* is a nitrifying bacterium of the genus Nitrospira, which plays an important role in the soil nitrogen cycle (Medriano et al. 2023). These findings collectively demonstrate that treatments involving *T. harzianum* monoculture (T1), garlic intercropping (T2), and their combination (T3) enhance beneficial soil microorganisms while suppressing harmful fungi.

This study further revealed that all treatments (T1, T2, and T3) enriched carbohydrate metabolism-related genes, with the combined treatment (T3) showing the highest enrichment. Functionally, this enrichment reflects microbial utilization of soil carbohydrates and amino acids for metabolic processes. Elevated functional gene abundance likely enhances the microbial capacity to assimilate these compounds, thereby increasing microbial diversity. Such shifts in gene abundance modulate microbial activity and drive ecological transformations (Paula et al. 2014). The GTs and GHs are critical for soil organic matter biosynthesis and decomposition (Sun and You 2021). The GHs hydrolyze glycosidic bonds to generate monosaccharides, oligosaccharides, or glycoconjugates, facilitating oligosaccharide synthesis, aromatic glycoside production, and amino acid/peptide glycosylation (Vuong et al. 2024; Xiao et al. 2019). The GTs are responsible for transferring sugar-based molecules and connecting them to other molecules such as proteins, oligosaccharides, and lipids (Cai et al. 2018; Chen et al. 2013; Huang et al. 2018). Together, these two types of enzymes laid the foundation for the formation, transport, and metabolism of carbohydrates. Among

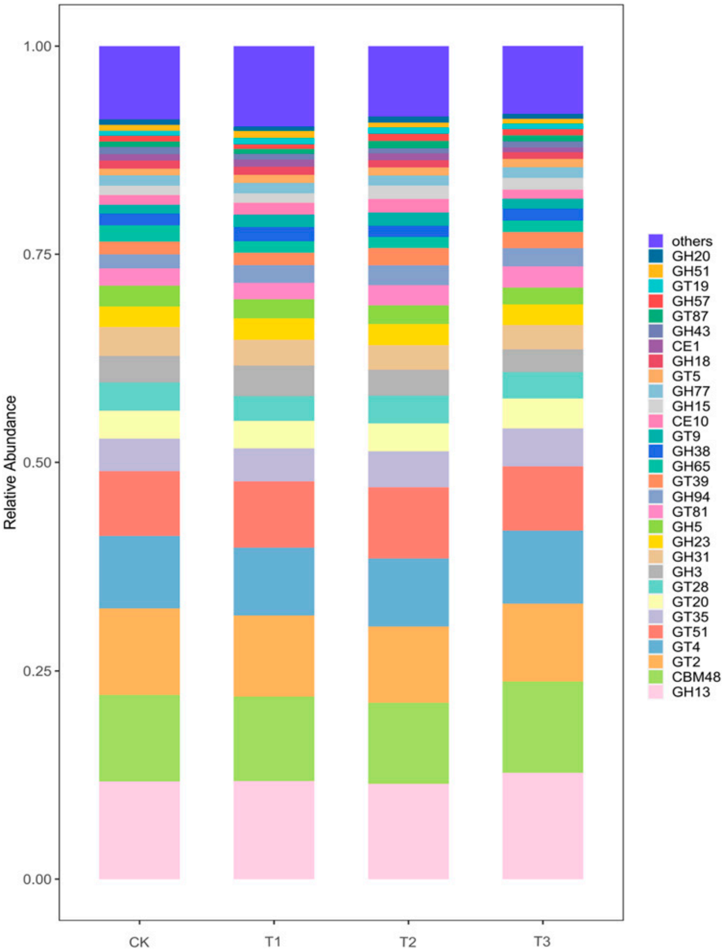

Fig. 13. Analysis of carbohydrate-active enzymes (CAZy) data.

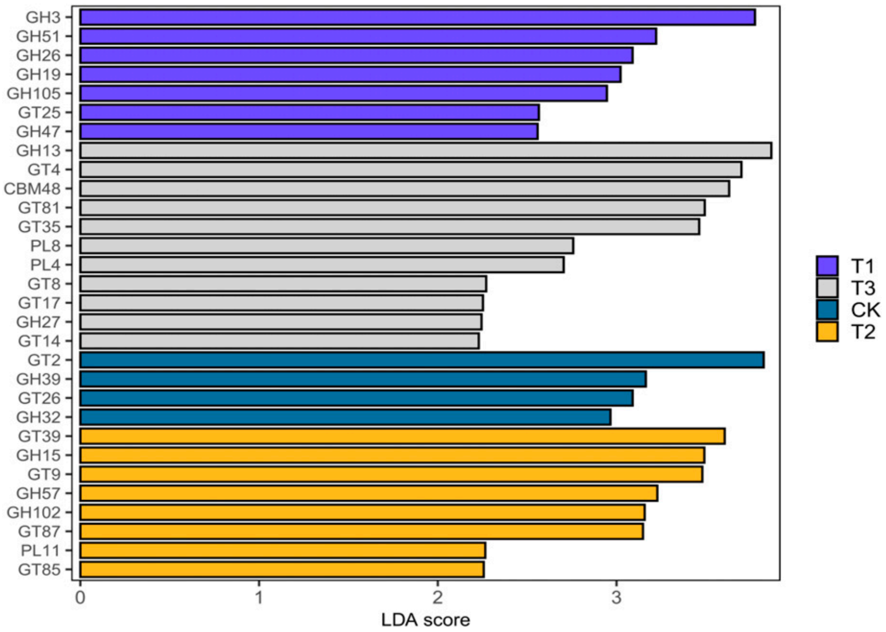

Fig. 14. LEfSe analyses of differential functions between groups.

them, the GH family is mainly involved in the degradation of cellulose and oligosaccharides, especially the hydrolysis of various glycosidic residues such as mannose, glucoside, and lactose (Nguyen et al. 2019). In soil ecosystems, microorganisms use nutrients derived from GH/GT activity, thus highlighting their role in organic carbon dynamics.

All treatments significantly increased soil microbial gene abundance linked to nitrogen and phosphorus cycling. The NHCC monoculture inoculated with *T. harzianum* significantly increased the abundance of K01113 (phoD) genes related to phosphorus nutrient activation and K00368 (nirK) and K15864 (nirS) genes related to denitrification. The NHCC–garlic intercropping with water significantly increased the abundance of the K01113 (phoD) gene related to phosphorus nutrient activation, K00370 (narG) and K15864 (nirS) genes related to denitrification, and K10944 (amoA) gene related to ammonia oxidation. The combined treatment (T3) markedly elevated the abundances of phosphorus nutrient activation genes K01113 (phoD), denitrification genes K00370 (narG), K00368 (nirK), K15864 (nirS), and ammonia oxidation genes K10944 (amoA). Wang et al. (2020) and Santos-Beneit (2015) identified *amoA*, *nirK*, *nirS*, and *narG* as key biomarkers for nitrogen-cycling microorganisms, while *phoD* regulates phosphorus uptake and metabolism. Wei et al. (2023) reported that *T. harzianum* increases bacterial *amoA* gene abundance in sweet sorghum rhizospheres. Intercropping systems elevated *nirS* and *phoD* abundances (Su et al. 2024). This study concluded that all treatments enhance nitrogen-related and phosphorus-related functional gene abundance in soil microbiota, with the combined treatment (T3) showing the broadest gene activation and monoculture inoculated with *T. harzianum* (T1) showing the least gene activation. Therefore, the combined treatment (T3) can be used to enhance nutrient absorption in continuous cropping systems, thereby boosting yield and quality.

All treatments promoted NHCC growth, increased soil available nitrogen, phosphorus, potassium, and exchangeable calcium, elevated leaf chlorophyll and soluble sugar content, and reduced POD, SOD, and MDA levels. The combined treatment (T3) exhibited the strongest growth-promoting effects on crop and soil quality, while monoculture inoculated with *T. harzianum* (T1) had the weakest impact. *T. harzianum* and garlic intercropping are established growth enhancers in diverse crops. Yedidia et al. (2001) found that *T. harzianum* significantly increased cucumber seedling emergence rate, shoot length, root length, root area, dry weight, and leaf area and promoted the absorption of copper, phosphorus, iron, zinc, and manganese in cucumber. Zhou et al. (2011) found that garlic and cucumber intercropping increased cucumber yield and improved the soil environment. As a commonly used biocontrol agent, *T. harzianum* is effective for alleviating the continuous cropping obstacles and promoting growth in a wide range of crops (Al-Shuaibi et al. 2024; Mao and Jiang 2021). The growth-promoting function of *T. harzianum*, which is mainly reflected in a variety of metabolites, including chitinase and cellulase, can be produced to inhibit the growth of pathogens and trigger the host defense system (Halifu et al. 2019). *T. harzianum* can dissolve phosphate, produce plant hormones, and promote plant growth under salt stress (Zhao and Zhang 2015). *T. harzianum* can synthesize phytohormones, produce vitamins, enhance soil nutrient solubility, increase nutrient uptake and translocation, and accelerate root development and carbohydrate metabolism

Table 1. Abundance of significantly different functional genes related to nitrogen and phosphorus nutrient cycling.

Function	KO	Gene name	CK	T1	T2	T3
Alkaline phosphatase	K01113	phoD	141.20 ± 2.88 b	162.70 ± 2.83 a	173.38 ± 2.57 a	179.45 ± 2.21 a
Ammonia oxidation	K10944	amoA	19.40 ± 1.88 b	20.58 ± 1.15 b	26.55 ± 0.80 a	27.24 ± 0.23 a
Nitrate reduction	K00370	narG	273.86 ± 3.82 b	250.53 ± 7.87 b	339.92 ± 3.98 a	353.74 ± 5.79 a
Nitrite reduction	K00368	nirK	381.74 ± 7.87 b	409.00 ± 7.47 a	372.97 ± 4.93 b	410.01 ± 6.79 a
Nitrite reduction	K15864	nirS	6.80 ± 1.27 b	14.91 ± 1.10 a	12.41 ± 1.34 a	13.58 ± 0.64 a

Data are means ± standard deviation. Different lowercase letters in the same row indicate significant differences between treatments ($P < 0.05$).

CK = control; KO = KEGG Orthology; T1 = NHCC monoculture inoculated with *Trichoderma harzianum*; T2 = NHCC–garlic intercropping with water; T3 = NHCC–garlic intercropping inoculated with *T. harzianum*.

Table 2. Changes in soil nutrients in nonheading Chinese cabbage (NHCC) under different treatments.

Treatments	Organic matter $g \cdot kg^{-1}$	Total phosphorus $g \cdot kg^{-1}$	Total potassium $g \cdot kg^{-1}$	Available nitrogen $mg \cdot kg^{-1}$	Available phosphorus $mg \cdot kg^{-1}$	Available potassium $mg \cdot kg^{-1}$	Exchangeable calcium $mg \cdot kg^{-1}$
CK	25.63 ± 1.42 a	0.86 ± 0.01 a	10.48 ± 0.02 a	73.61 ± 0.56 d	26.50 ± 1.47 b	46.26 ± 1.48 b	1406.89 ± 1.16 c
T1	26.47 ± 0.61 a	0.87 ± 0.01 a	10.43 ± 0.02 a	82.26 ± 1.16 c	27.33 ± 0.54 b	50.25 ± 2.42 a	1413.59 ± 0.80 c
T2	26.10 ± 0.84 a	0.89 ± 0.02 a	10.05 ± 0.02 a	90.59 ± 1.17 b	24.10 ± 1.17 b	51.47 ± 1.11 a	1470.77 ± 1.16 b
T3	27.21 ± 2.12 a	0.90 ± 0.03 a	10.22 ± 0.01 a	96.94 ± 1.16 a	36.46 ± 0.22 a	51.27 ± 2.02 a	1519.42 ± 0.53 a

Data are means ± standard deviation. Different lowercase letters in the same row indicate significant differences between treatments ($P < 0.05$).

CK = control; T1 = NHCC monoculture inoculated with *Trichoderma harzianum*; T2 = NHCC–garlic intercropping with water; T3 = NHCC–garlic intercropping inoculated with *T. harzianum*.

Table 3. Growth indexes of nonheading Chinese cabbage (NHCC) under different treatments.

Treatments	Plant ht (cm)	Maximum root length (cm)	Leaf length (cm)	Leaf width (cm)	Fresh wt (g)
CK	22.98 ± 0.67 c	8.54 ± 0.84 b	20.41 ± 0.82 d	9.18 ± 0.90 c	20.80 ± 1.67 c
T1	25.62 ± 0.40 bc	9.73 ± 0.75 ab	22.80 ± 0.65 c	10.81 ± 0.41 b	37.59 ± 1.77 b
T2	27.10 ± 0.51 b	8.99 ± 0.30 ab	25.32 ± 0.62 b	11.63 ± 0.51 b	38.81 ± 1.18 ab
T3	33.33 ± 0.47 a	10.42 ± 0.09 a	31.11 ± 0.41 a	17.42 ± 0.36 a	42.68 ± 1.28 a

Data are means ± standard deviation. Different lowercase letters in the same row indicate significant differences between treatments ($P < 0.05$).

CK = control; T1 = NHCC monoculture inoculated with *Trichoderma harzianum*; T2 = NHCC–garlic intercropping with water; T3 = NHCC–garlic intercropping inoculated with *T. harzianum*.

Table 4. Physiological indexes of nonheading Chinese cabbage (NHCC) under different treatments.

Treatments	Chlorophyll $mg \cdot g^{-1}$	Soluble sugar $mg \cdot g^{-1}$	Soluble protein $mg \cdot g^{-1}$	POD µ/(g·min)	SOD $U \cdot g^{-1}$	MDA $nmol \cdot g^{-1}$
CK	1.02 ± 0.05 b	2.87 ± 0.08 b	7.29 ± 0.05 a	104.39 ± 1.23 a	369.31 ± 3.25 a	15.78 ± 0.11 a
T1	1.03 ± 0.04 b	2.40 ± 0.04 b	6.38 ± 0.06 b	111.97 ± 1.14 a	348.37 ± 2.78 b	13.17 ± 0.09 c
T2	1.12 ± 0.06 ab	4.55 ± 0.07 a	6.39 ± 0.07 b	77.12 ± 1.07 b	352.10 ± 3.16 b	14.56 ± 1.23 b
T3	1.17 ± 0.06 a	4.12 ± 0.06 a	5.71 ± 0.05 c	88.64 ± 1.05 b	329.99 ± 3.04 c	11.33 ± 1.15 d

Data are means ± standard deviation. Different lowercase letters in the same row indicate significant differences between treatments ($P < 0.05$).

CK = control; MDA = malondialdehyde; POD = peroxidase; SOD = superoxide dismutase; T1 = NHCC monoculture inoculated with *Trichoderma harzianum*; T2 = NHCC–garlic intercropping with water; T3 = NHCC–garlic intercropping inoculated with *T. harzianum*.

(Yedidia et al. 2001). Garlic, a common *Allium* species in intercropping systems, produces root exudates that enhance the growth of continuous NHCC at optimal concentrations (Cheng et al. 2011). The growth-promoting effects of *Allium* plants on continuous cropping systems are attributed to antimicrobial and insect-repellent properties of root exudates (Khan et al. 2011; Lai et al. 2011; Mogahed 2003; Portz et al. 2008), allelochemical-mediated enhancement of root antioxidant enzyme activity, reduction of MDA content, thereby improving root vitality (Cheng et al. 2020), and increased photosynthetic pigment content and photosynthetic efficiency in continuous cropping plants (Xiao et al. 2019). This study demonstrated that NHCC–garlic intercropping combined with *T. harzianum* (T3) exerted the strongest growth-promoting effects on NHCC. *Trichoderma*, a widely used biocontrol agent, exhibits limited soil competitiveness and requires organic nutrients for colonization (Miranda et al. 2006). Garlic enriches soil organic matter, available nitrogen, phosphorus, and potassium, and it enhances urease, phosphatase, and sucrase activity (Du et al. 2017; Xiao et al. 2013, 2019). The increase in these substances provides a large amount of organic nutrients to *T. harzianum*, which is more favorable for its colonization. Therefore, the growth-promoting effect of NHCC–garlic intercropping inoculated with *T. harzianum* was the best.

In summary, NHCC monoculture inoculated with *T. harzianum*, NHCC–garlic intercropping with water, and NHCC–garlic intercropping inoculated with *T. harzianum* can promote the growth of NHCC and enhance the NHCC quality and rhizosphere soil quality in different degrees. A metagenomic analysis further revealed that all treatments promoted beneficial microorganisms, suppressed pathogenic fungi, enriched carbohydrate metabolism-related genes, and amplified nitrogen-cycling and phosphorus-cycling gene abundance. The combined treatment (T3) exhibited the greatest effects, while *T. harzianum* monoculture (T1) showed the weakest effects.

References Cited

Abbasi MK, Sharif S, Kazmi M, Sultan T, Aslam M. 2011. Isolation of plant growth promoting rhizobacteria from wheat rhizosphere and their effect on improving growth, yield and nutrient uptake of plants. Plant Biosyst. 145(1):159–168. https://doi.org/10.1080/11263504.2010.542318.

Ahmad I, Zhu G, Zhou G, Song X, Hussein Ibrahim ME, Ibrahim Salih EG. 2022. Effect of N on growth, antioxidant capacity, and chlorophyll content of sorghum. Agronomy. 12(2):501. https://doi.org/10.3390/agronomy12020501.

Al-Shuaibi BK, Kazerooni EA, Al-Maqbali D, Al-Kharousi M, Al-Yahya'ei MN, Hussain S, Velazhahan R, Al-Sadi AM. 2024. Biocontrol potential of Trichoderma ghanense and Trichoderma citrinoviride toward *Pythium aphanidermatum*. J Fungi (Basel). 10(4):284. https://doi.org/10.3390/jof10040284.

Boulahouat S, Cherif-Silini H, Silini A, Bouket AC, Luptakova L, Alenezi FN, Belbahri L. 2023. Biocontrol efficiency of rhizospheric *Bacillus* against the plant pathogen *Fusarium oxysporum*: A promising approach for sustainable agriculture. Microbiol Res (Pavia). 14(3):892–908. https://doi.org/10.3390/microbiolres14030062.

Cai H, Zhang T, Zhang Q, Luo J, Cai C, Mao J. 2018. Microbial diversity and chemical analysis of the starters used in traditional Chinese sweet rice wine. Food Microbiol. 73:319–326. https://doi.org/10.1016/j.fm.2018.02.002.

Cantarel BL, Coutinho PM, Rancurel C, Bernard T, Lombard V, Henrissat B. 2009. The Carbohydrate-Active EnZymes database (CAZy): An expert resource for glycogenomics. Nucleic Acids Res. 37(1S):D233–D238. https://doi.org/10.1093/nar/gkn663.

Cao X, Zhang N, Zeng X, Lan Q, Ma N, Wu C. 2022. Effects of biochar and Trichoderma on bacterial community diversity in continuous cropping soil. Hortic Environ Biotechnol. 63(1):1–12. https://doi.org/10.1007/s13580-021-00373-8.

Chen B, Yang H, Song W, Liu C, Xu J, Zhao W, Zhou Z. 2016. Effect of N fertilization rate on soil alkali-hydrolyzable N, subtending leaf N concentration, fiber yield, and quality of cotton. Crop J. 4:323–330. https://doi.org/10.1016/j.cj.2016.03.006.

Chen S, Xu Y, Qian MC. 2013. Aroma characterization of Chinese rice wine by gas chromatography–olfactometry, chemical quantitative analysis, and aroma reconstitution. J Agric Food Chem. 61(47):11295–11302. https://doi.org/10.1021/jf4030536.

Chen Y, Li S, Liu N, He H, Cao X, Lv C, Zhang K, Dai J. 2021. Effects of different types of microbial inoculants on available nitrogen and phosphorus, soil microbial community, and wheat growth in high-P soil. Environ Sci Pollut Res Int. 28(18):23036–23047. https://doi.org/10.1007/s11356-020-12203-y.

Cheng F, Ali M, Liu C, Deng R, Cheng Z. 2020. Garlic allelochemical diallyl disulfide alleviates autotoxicity in the root exudates caused by long-term continuous cropping of tomato. J Agric Food Chem. 68(42):11684–11693. https://doi.org/10.1021/acs.jafc.0c03894.

Cheng Z, Wang H, Xiao X, Khan MA. 2011. Allelopathic effects of decomposing garlic stalk on some vegetable crops. Afr J Biotechnol. 10(69): 15514–15520. https://www.cabidigitallibrary.org/doi/full/10.5555/20113390659.

Dos Santos Fonseca J, Altoé LSC, D, Carvalho LM, De Freitas Soares FE, Braga FR, D, Araújo JV. 2023. Nematophagous fungus *Pochonia chlamydosporia* to control parasitic diseases in animals. Appl Microbiol Biotechnol. 107(12): 3859–3868. https://doi.org/10.1007/s00253-023-12525-0.

Du L, Huang B, Du N, Guo S, Shu S, Sun J. 2017. Effects of garlic/cucumber relay intercropping on soil enzyme activities and the microbial environment in continuous cropping. HortScience. 52(1):78–84. https://doi.org/10.21273/HORTSCI11442-16.

Elnahal ASM, El-Saadony MT, Saad AM, Desoky ESM, El-Tahan AM, Rady MM, AbuQamar SF, El-Tarabily KA. 2022. The use of microbial inoculants for biological control, plant growth promotion, and sustainable agriculture: A review. Eur J Plant Pathol. 162(4):759–792. https://doi.org/10.1007/s10658-021-02393-7.

Erazo JG, Palacios SA, Pastor N, Giordano FD, Rovera M, Reynoso MM, Venisse JS, Torres AM. 2021. Biocontrol mechanisms of *Trichoderma harzianum* ITEM 3636 against peanut brown root rot caused by *Fusarium solani* RC

386. Biol Control. 164:104774. https://doi.org/10.1016/j.biocontrol.2021.104774.

Fang S, Hou X, Liang X. 2021. Response mechanisms of plants under saline-alkali stress. Front Plant Sci. 12:667458. https://doi.org/10.3389/fpls.2021.667458.

Fu L, Niu B, Zhu Z, Wu S, Li W. 2012. CD-HIT: Accelerated for clustering the next-generation sequencing data. Bioinformatics. 28(23):3150–3152. https://doi.org/10.1093/bioinformatics/bts565.

Gao X, Xiao Y, Deng L, Li Q, Wang C, Li B, Deng O, Zeng M. 2019. Spatial variability of soil total nitrogen, phosphorus and potassium in Renshou County of Sichuan Basin, China. J Integr Agric. 18(2):279–289. https://doi.org/10.1016/S2095-3119(18)62069-6.

Halifu S, Deng X, Song X, Song R. 2019. Effects of two *Trichoderma* strains on plant growth, rhizosphere soil nutrients, and fungal community of *Pinus sylvestris* var. *mongolica* annual seedlings. Forests. 10(9):758. https://doi.org/10.3390/f10090758.

Hamid S, Ahmad I, Akhtar MJ, Iqbal MN, Shakir M, Tahir M, Rasoo A, Sattar A, Khalid M, Ditta A, Zhu B. 2021. *Bacillus subtilis* Y16 and biogas slurry enhanced potassium to sodium ratio and physiology of sunflower (*Helianthus annuus* L.) to mitigate salt stress. Environ Sci Pollut Res Int. 28(29):38637–38647. https://doi.org/10.1007/s11356-021-13419-2.

Han T, Cai A, Liu K, Huang J, Wang B, Li D, Qaswar M, Feng G, Zhang H. 2019. The links between potassium availability and soil exchangeable calcium, magnesium, and aluminum are mediated by lime in acidic soil. J Soils Sediments. 19(3):1382–1392. https://doi.org/10.1007/s11368-018-2145-6.

Hartmann M, Six J. 2023. Soil structure and microbiome functions in agroecosystems. Nat Rev Earth Environ. 4(1):4–18. https://doi.org/10.1038/s43017-022-00366-w.

Hashem A, Tabassum B, Fathi Abd Allah E. 2019. Bacillus subtilis: A plant-growth promoting rhizobacterium that also impacts biotic stress. Saudi J Biol Sci. 26(6):1291–1297. https://doi.org/10.1016/j.sjbs.2019.05.004.

Hou Y, Zhou B, Wang Q. 2018. Effects of Bacillus subtilis on Evaporation of Soil Surface and Water and Salt Dsitritution in Saline-alkali Soil. J Soil Water Conserv. 32(2):306–311. https://doi.org/10.13870/j.cnki.stbcxb.2018.02.045.

Huang Z-R, Hong J-L, Xu J-X, Li L, Guo W-L, Pan Y-Y, Chen S-J, Bai W-D, Rao P-F, Ni L, Zhao L-N, Liu B, Lv X-C. 2018. Exploring core functional microbiota responsible for the production of volatile flavour during the traditional brewing of Wuyi Hong Qu glutinous rice wine. Food Microbiol. 76:487–496. https://doi.org/10.1016/j.fm.2018.07.014.

Hyatt D, Chen G, LoCascio PF, Land ML, Larimer FW, Hauser LJ. 2010. Prodigal: Prokaryotic gene recognition and translation initiation site identification. BMC Bioinformatics. 11(1):1–11. https://doi.org/10.1186/1471-2105-11-119.

Irani H, ValizadehKaji B, Naeini MR. 2021. Biostimulant-induced drought tolerance in grapevine is associated with physiological and biochemical changes. Chem Biol Technol Agric. 8(1):1–13. https://doi.org/10.1186/s40538-020-00200-9.

Jaber LR, Enkerli J. 2016. Effect of seed treatment duration on growth and colonization of Vicia faba by endophytic *Beauveria bassiana* and *Metarhizium brunneum*. Biol Control. 103:187–195. https://doi.org/10.1016/j.biocontrol.2016.09.008.

Kermah M, Franke AC, Adjei-Nsiah S, Ahiabor BDK, Abaidoo RC, Giller KE. 2017. Maize-grain legume intercropping for enhanced resource use efficiency and crop productivity in the Guinea savanna of northern Ghana. Field Crops Res. 213:38–50. https://doi.org/10.1016/j.fcr.2017.07.008.

Khan MA, Cheng Z, Xiao X, Khan AR, Ahmed SS. 2011. Ultrastructural studies of the inhibition effect against *Phytophthora capsici* of root exudates collected from two garlic cultivars along with their qualitative analysis. Crop Prot. 30(9):1149–1155. https://doi.org/10.1016/j.cropro.2011.04.013.

Krey T, Caus M, Baum C, Ruppel S, Eichler-Löbermann B. 2011. Interactive effects of plant growth-promoting rhizobacteria and organic fertilization on P nutrition of *Zea mays* L. and *Brassica napus* L. Z Pflanzenernähr Bodenk. 174(4):602–613. https://doi.org/10.1002/jpln.200900349.

Lai R, You M, Lotz LAP, Vasseur L. 2011. Response of green peach aphids and other arthropods to garlic intercropped with tobacco. Agron J. 103(3):856–863. https://doi.org/10.2134/agronj2010.0404.

Langmead B, Salzberg SL. 2012. Fast gapped-read alignmentwith Bowtie 2. Nat Methods. 9(4):357–359. https://doi.org/10.1038/nmeth.1923.

Lei H, Wang J, Hu Q, Li C, Mo M, Zhang K, Li G, Zhao P. 2023. 2-Furoic acid associated with the infection of nematodes by *Dactylellina haptotyla* and its biocontrol potential on plant root-knot nematodes. Microbiol Spectr. 11(5):e01896-23. https://doi.org/10.1128/spectrum.01896-23.

Li D, Liu C, Luo R, Sadakane K, Lam TW. 2015. MEGAHIT: An ultra-fast single-node solution for large and complex metagenomics assembly via succinct *de Bruijn* graph. Bioinformatics. 31(10):1674–1676. https://doi.org/10.1093/bioinformatics/btv033.

Li D, Luo R, Liu CM, Leung CM, Ting HF, Sadakane K, Yamashita H, Lam TK. 2016. MEGAHIT v1. 0: A fast and scalable metagenome assembler driven by advanced methodologies and community practices. Methods. 102:3–11. https://doi.org/10.1016/j.ymeth.2016.02.020.

Li Y, Liu G, Ma L, Liu T, Zhang C, Xiao D, Zheng H, Chen F, Hou X. 2020. A chromosome-level reference genome of non-heading Chinese cabbage [*Brassica campestris* (syn. *Brassica rapa*) ssp. *chinensis*]. Hortic Res. 7(1):212–224. https://doi.org/10.1038/s41438-020-00449-z.

Liu Q, Yang J, Ahmed W, Wan X, Wei L, Ji G. 2022. Exploiting the antibacterial mechanism of phenazine substances from *Lysobacter antibioticus* 13-6 against *Xanthomonas oryzae* pv. *oryzicola*. J Microbiol. 60(5):496–510. https://doi.org/10.1007/s12275-022-1542-0.

Mao T, Jiang X. 2021. Changes in microbial community and enzyme activity in soil under continuous pepper cropping in response to *Trichoderma hamatum* MHT1134 application. Sci Rep. 11(1):21585. https://doi.org/10.1038/s41598-021-00951-x.

Marquez N, Giachero ML, Declerck S, Ducasse DA. 2021. *Macrophomina phaseolina*: General characteristics of pathogenicity and methods of control. Front Plant Sci. 12:634397. https://doi.org/10.3389/fpls.2021.634397.

Medriano CA, Chan A, De Sotto R, Bae S. 2023. Different types of land use influence soil physiochemical properties, the abundance of nitrifying bacteria, and microbial interactions in tropical urban soil. Sci Total Environ. 869:161722. https://doi.org/10.1016/j.scitotenv.2023.161722.

Miranda MEA, Estrella AH, Cabriales JJP. 2006. Colonization of the rhizosphere, rhizoplane and endorhiza of garlic (*Allium sativum* L.) by strains of *Trichoderma harzianum* and their capacity to control allium white-rot under field conditions. SBB. 38(7):1823–1830. https://doi.org/10.1016/j.soilbio.2005.11.036.

Mogahed MI. 2003. Influence of intercropping on population dynamics of major insect-pests of potato (*Solanum tuberosum*) in North Sinai Governorate, Egypt. Indian J Agric Sci. 73(10):546–549. https://www.cabidigitallibrary.org/doi/full/10.5555/20043029929.

Nguyen SN, Flores A, Talamantes D, Dar F, Valdez A, Schwans J, Berlemont R. 2019. GeneHunt for rapid domain-specific annotation of glycoside hydrolases. Sci Rep. 9(1):10137. https://doi.org/10.1038/s41598-019-46290-w.

Patkowska E, Mielniczuk E, Jamiołkowska A, Skwaryło-Bednarz B, Błażewicz-Woźniak M. 2020. The influence of *Trichoderma harzianum* Rifai T-22 and other biostimulants on rhizosphere beneficial microorganisms of carrot. Agronomy. 10(11):1637. https://doi.org/10.3390/agronomy10111637.

Paula FS, Rodrigues JL, Zhou J, Wu L, Mueller RC, Mirza BS, Bohannan BJM, Nüsslein K, Deng Y, Tiedje JM, Pellizari VH. 2014. Land use change alters functional gene diversity, composition and abundance in Amazon forest soil microbial communities. Mol Ecol. 23(12):2988–2999. https://doi.org/10.1111/mec.12786.

Portz D, Koch E, Slusarenko AJ. 2008. Effects of garlic (*Allium sativum*) juice containing allicin on *Phytophthora infestans* and downy mildew of cucumber caused by *Pseudoperonospora cubensis*. In: Lebeda A, Spencer-Phillips PTN, Cooke BM. (eds). The Downy Mildews - Genetics, Molecular Biology and Control. Springer, Dordrecht, The Netherlands. https://doi.org/10.1007/978-1-4020-8973-2_15.

Ren N, Wang Y, Ye Y, Zhao Y, Huang Y, Fu W, Chu X. 2020. Effects of continuous nitrogen fertilizer application on the diversity and composition of rhizosphere soil bacteria. Front Microbiol. 11:1948. https://doi.org/10.3389/fmicb.2020.01948.

Santos-Beneit F. 2015. The Pho regulon: A huge regulatory network in bacteria. Front Microbiol. 6:402. https://doi.org/10.3389/fmicb.2015.00402.

Su H, Lai H, Gao F, Zhang R, Wu S, Ge F, Li Y, Yao H. 2024. The proliferation of beneficial bacteria influences the soil C, N, and P cycling in the soybean–maize intercropping system. Environ Sci Pollut Res Int. 31(17):25688–25705. https://doi.org/10.1007/s11356-024-32851-8.

Sun S, You C. 2021. Disaccharide phosphorylases: Structure, catalytic mechanisms and directed evolution. Synth Syst Biotechnol. 6(1):23–31. https://doi.org/10.1016/j.synbio.2021.01.004.

Villar E, Farrant GK, Follows M, Garczarek L, Speich S, Audic S, Bittner L, Blanke B, Brum JR, Brunet C, Casotti R, Chase A, Dolan JR, d'Ortenzio F, Gattuso J-P, Grima N, Guidi L, Hill CN, Jahn O, Jamet J-L, Le Goff H, Lepoivre C, Malviya S, Pelletier E, Romagnan J-B, Roux S, Santini S, Scalco E, Schwenck SM, Tanaka A, Testor P, Vannier T, Vincent F, Zingone A, Dimier C, Picheral M, Searson S, Kandels-Lewis S, Acinas SG, Bork P, Boss E, de Vargas C, Gorsky G, Ogata H, Pesant S, Sullivan MB, Sunagawa S, Wincker P, Karsenti E, Bowler C, Not F, Hingamp P, Iudicone D. 2015. Environmental characteristics of Agulhas rings affect interocean plankton transport. Science. 348(6237):1261447. https://doi.org/10.1126/science.1261447.

Vuong TV, Aghajohari M, Feng X, Woodstock AK, Nambiar DM, Sleiman ZC, Urbanowicz BR, Master ER. 2024. Enzymatic routes to designer hemicelluloses for use in biobased materials. JACS Au. 4(11):4044–4065. https://doi.org/10.1021/jacsau.4c00469.

Wang F, Wang X, Zhao R, Zhang L, Li S, Zhang N, Han H. 2024. Differences in the soil prokaryotic microbiome during continuous and single cultivation of three varieties of chinese cabbage. Eurasian Soil Sci. 57(10):1674–1687. https://doi.org/10.1134/S1064229323603566.

Wang J, Mu H, Liu S, Qi S, Mou S. 2024. Effects of *Trichoderma harzianum* fertilizer on growth and rhizosphere microbial community of continuous cropping *Lagenaria siceraria*. Microorganisms. 12(10):1987. https://doi.org/10.3390/microorganisms12101987.

Wang Y, Huang X, Huang X, Su W, Hao Y, Liu H, Chen R, Song S. 2022. *BcSOC1* promotes bolting and stem elongation in flowering chinese cabbage. Int J Mol Sci. 23(7):3459. https://doi.org/10.3390/ijms23073459.

Wang YY, Qi L, Huang R, Wang FH, Wang ZF, Gao M. 2020. Characterization of denitrifying community for application in reducing nitrogen: A comparison of *nirK* and *nirS* gene diversity and abundance. Appl Biochem Biotechnol. 192(1): 22–41. https://doi.org/10.1007/s12010-020-03250-9.

Wei Y, Yang H, Hu J, Li H, Zhao Z, Wu Y, Li J, Zhou Y, Yang K, Yang H. 2023. *Trichoderma harzianum* inoculation promotes sweet sorghum growth in the saline soil by modulating rhizosphere available nutrients and bacterial community. Front Plant Sci. 14:1258131. https://doi.org/10.3389/fpls.2023.1258131.

Xia Z, Kong C, Chen L, Wang P, Long S. 2016. A broadleaf species enhances an autotoxic conifers growth through belowground chemical interactions. Ecology. 97(9):2283–2292. https://doi.org/10.1002/ecy.1465.

Xiao X, Cheng Z, Lv J, Xie J, Ma N, Yu J. 2019. A green garlic (*Allium sativum* L.) based intercropping system reduces the strain of continuous monocropping in cucumber (*Cucumis sativus* L.) by adjusting the micro-ecological environment of soil. PeerJ. 7:e7267. https://doi.org/10.7717/peerj.7267.

Xiao X, Cheng Z, Meng H, Khan MA, Li H. 2012. Intercropping with garlic alleviated continuous cropping obstacle of cucumber in plastic tunnel. J Agric Scand Sect B Soil Plant Sci. 62(8):696–705. https://doi.org/10.1080/09064710.2012.697571.

Xiao X, Cheng Z, Meng H, Liu L, Li H, Dong Y. 2013. Intercropping of green garlic(*Allium sativum* L.) induces nutrient concentration changes in the soil and plants in continuously cropped cucumber (*Cucumis sativus* L.) in a plastic tunnel. PLoS One. 8(4):e62173. https://doi.org/10.1371/journal.pone.0062173.

Yang X, Yang L, Shi Y, Lei F, Dong L, Zheng C, Zhang D, Sun L, Xie A, Sun X. 2023. Analysis of exogenous lactic acid bacteria on growth and development of different herbaceous peony varieties and rhizosphere soil nutrients. Chem Biol Technol Agric. 10(1):144. https://doi.org/10.1186/s40538-023-00516-2.

Yedidia I, Srivastva AK, Kapulnik Y, Chet I. 2001. Effect of *Trichoderma harzianum* on microelement concentrations and increased growth of cucumber plants. Plant Soil. 235(2):235–242. https://doi.org/10.1023/A:1011990013955.

Zeng J, Liu J, Lu C, Ou X, Luo K, Li C, He M, Zhang H, Yan H. 2020. Intercropping with turmeric or ginger reduce the continuous cropping obstacles that affect *Pogostemon cablin* (patchouli). Front Microbiol. 11:579719. https://doi.org/10.3389/fmicb.2020.579719.

Zhang L, Chen F, Zeng Z, Xu M, Sun F, Yang L, Bi X, Lin Y, Gao Y, Hao H, Yi W, Li M, Xie Y. 2021. Advances in metagenomics and its application in environmental microorganisms. Front Microbiol. 12:766364. https://doi.org/10.3389/fmicb.2021.766364.

Zhao L, Zhang Y. 2015. Effects of phosphate solubilization and phytohormone production of *Trichoderma asperellum* Q1 on promoting cucumber growth under salt stress. J Integr Agric. 14(8):1588–1597. https://doi.org/10.1016/S2095-3119(14)60966-7.

Zhou X, Jia X, Zhang Z, Chen K, Wang L, Chen H, Yang Z, Li C, Zhao L. 2022. AgNPs seed priming accelerated germination speed and altered nutritional profile of Chinese cabbage. Sci Total Environ. 808:151896. https://doi.org/10.1016/j.scitotenv.2021.151896.

Zhou X, Yu G, Wu F. 2011. Effects of intercropping cucumber with onion or garlic on soil enzyme activities, microbial communities and cucumber yield. Eur J Soil Biol. 47(5):279–287. https://doi.org/10.1016/j.ejsobi.2011.07.001.